

## **Experimental Reconstitution of Chronic ER Stress in the Liver Reveals Feedback Suppression of Bip mRNA Expression**

Javier A. Gomez<sup>1</sup> and D. Thomas Rutkowski<sup>2,3\*</sup>

<sup>1</sup>Graduate Program in Molecular and Cellular Biology and <sup>2</sup>Departments of Anatomy and Cell Biology and <sup>3</sup>Internal Medicine, University of Iowa Carver College of Medicine, Iowa City, IA 52242

\*corresponding author: [thomas-rutkowski@uiowa.edu](mailto:thomas-rutkowski@uiowa.edu)

Running title: BiP suppression during chronic stress

## Abstract

ER stress is implicated in many chronic diseases, but very little is known about how the unfolded protein response (UPR) responds to persistent ER stress *in vivo*. Here, we experimentally reconstituted chronic ER stress in the mouse liver, using repeated injection of a low dose of the ER stressor tunicamycin. Paradoxically, this treatment led to feedback-mediated suppression of a select group of mRNAs, including those encoding the ER chaperones BiP and GRP94. This suppression was due to both silencing of the ATF6 $\alpha$  pathway of UPR-dependent transcription and enhancement of mRNA degradation, most likely via regulated IRE1-dependent decay (RIDD). The suppression of *Bip* mRNA was phenocopied by ectopic overexpression of BiP protein, and was also observed in obese mice. Our findings suggest that persistent cycles of UPR activation and deactivation create an altered, quasi-stable setpoint for UPR-dependent transcriptional regulation—an outcome that could be relevant to conditions such as metabolic syndrome.

## Introduction

The western obesity epidemic has exposed one of the consequences of modernity: the increasing prevalence of non-infectious chronic diseases that progress down increasingly irreversible paths over the course of years to decades. Diabetes, atherosclerosis, hypertension, steatohepatitis, and the like join neurodegenerative disorders, cancers, lung disease and other chronic diseases in driving morbidity and mortality in the western world (Ezzati *et al.*, 2002). As a class, these diseases necessarily entail a *gradual* deterioration of cellular and organ function, rather than an acute collapse. Thus, treating or reversing them requires understanding how persistent but otherwise modest stimuli alter the activity of key cellular pathways.

One cellular pathway increasingly implicated in the progression of a number of chronic diseases is the Unfolded Protein Response (UPR). The UPR is activated by disruption of the protein folding capacity of the endoplasmic reticulum, otherwise known as “ER stress” (Walter and Ron, 2011). Unremitted ER stress and/or a dysregulated UPR appear to contribute to hepatic steatosis and steatohepatitis (Malhi and Kaufman, 2011), atherosclerosis (Zhou and Tabas, 2013), colitis and inflammatory bowel disease (Kaser *et al.*, 2013), hypertension (Young and Davisson, 2015), and many others. As an organelle that carries out several essential cellular processes (protein processing, calcium storage, lipogenesis, certain metabolic steps, etc.) and that is physically and functionally intertwined with many other critical cellular pathways, the ER is sensitive to a range of diverse stimuli. For example, ER stress is observed in the livers of obese

mice (Özcan *et al.*, 2004), and this response has been attributed to an excess load of nascent client proteins in the organelle due to nutrient-mediated stimulation of mTOR activity (Özcan *et al.*, 2008). Other physiological stimuli that elicit ER stress include nutritional status and the activity of metabolic pathways (Oyadomari *et al.*, 2008; Tyra *et al.*, 2012; Shao *et al.*, 2014), differentiation cues (Iwakoshi *et al.*, 2003; van Anken *et al.*, 2003; Lee *et al.*, 2005), inflammatory signals (Zhang *et al.*, 2006; Hotamisligil, 2010), and many, many others. While the UPR is capable of responding to excessive ER stress by initiating cell death cascades (Sano and Reed, 2013), chronic stress is instead likely to result not in cell death (at least not for most cells, most of the time), but instead a persistent burden on ER function that must be accommodated by the UPR. And yet, for many chronic diseases in which ER stress is implicated, it is not clear whether disease results from a UPR that becomes progressively dysregulated and thus responds *inappropriately*, or whether the UPR becomes progressively neutered and simply becomes increasingly *unresponsive*.

Experimental manipulation of the UPR has sketched the framework of a canonical UPR that is initiated by three ER-resident proteins and that culminates in transcriptional augmentation of the ER protein processing capacity and other non-transcriptional mechanisms to alleviate ER load. The inositol-requiring enzyme 1 $\alpha$  (IRE1 $\alpha$ ) pathway results in both the production of the XBP1 transcription factor (Yoshida *et al.*, 2001; Calton *et al.*, 2002; Lee *et al.*, 2002) and the degradation of ER-associated mRNAs in a process known as Regulated IRE1-Dependent Decay via the IRE1 endonuclease activity (Hollien and Weissman, 2006; Hollien *et al.*, 2009). The PKR-like



endoplasmic reticulum kinase (PERK) stimulates production of the ATF4 transcription factor (Harding *et al.*, 2000) and also transiently reduces ER protein load by phosphorylation of the translation initiation factor eIF2 $\alpha$  (Shi *et al.*, 1998; Harding *et al.*, 1999). ATF6 (comprising both  $\alpha$  and  $\beta$  paralogs) initiates the third pathway when ATF6 is itself cleaved by regulated intramembrane proteolysis in the Golgi, liberating a transcriptionally active N-terminal fragment (Ye *et al.*, 2000). These pathways are all robustly activated by acute exposure of cells to high doses of ER stress-inducing drugs, which is an effective tool for understanding what the system is capable of but not as effective for understanding how the cellular response to chronic stress differs from these canonical pathways.

Evidence for the involvement of ER stress in chronic diseases in general comes from two lines of investigation: detecting markers of ER stress in the affected tissues of human patients or mouse models thereof, and observing disease-like phenotypes in mice with genetic ablations of UPR signaling pathways. Yet while studies of this sort provide *prima facie* evidence for UPR involvement, they do not address how the UPR becomes dysregulated during chronic disease, if in fact it even does. Further, animal models of chronic diseases such as those associated with obesity tend to influence innumerable cellular pathways and make it difficult to isolate the effects of ER stress *per se* from the many other confounding factors.

With these considerations in mind, we set out to address how the UPR responds to chronic stress *in vivo*. Following the example of our previous work *in vitro* (Rutkowski *et al.*, 2006), here we describe how UPR signaling in the liver becomes altered during

repeated exposure to stress, the mechanisms by which these alterations occur, and their potential relevance to liver dysfunction during obesity.

## Results

### *The liver adapts to persistent ER stress*

Our first step in experimentally reconstituting chronic ER stress was to identify conditions that were as specific as possible in perturbing ER function with minimal pleiotropic effects, and were sufficient to activate the UPR without causing overt toxicity. In doing so, we hoped to be able to understand how the UPR responds to chronic stress, divorced from the confounding influences of chronic diseases on other cellular pathways. Toward this end, we used tunicamycin (TM) to induce ER stress *in vivo*; TM blocks N-linked glycosylation, an ER-specific protein modification. It has few known off-target effects, most prominently targets the kidneys and the liver, and is not lethal in wild-type animals at even relatively high doses (Foufelle and Fromenty, 2016). Its effects on the liver can also be mimicked, albeit less readily, by other agents that elicit ER stress in that organ (Rutkowski *et al.*, 2008; Chikka *et al.*, 2013), further justifying its use here. Following an approach analogous to one we described previously (Rutkowski *et al.*, 2006), we looked for a dose of TM that was capable of inducing the UPR, but that was significantly less toxic than the common experimental dose of 1 mg/kg—which is known to elicit hepatocellular death and inflammation (Foufelle and Fromenty, 2016). Using qRT-PCR to detect changes in expression of the UPR sentinel genes *Bip* and *Chop*, we found that doses of TM below 0.1 mg/kg were capable of eliciting attenuated UPR activation (**Figure 1A**).

Based on this finding, we chose 0.025 mg/kg as the dose most likely to be tolerated long-term by mice without leading to significant toxicity, and we used it as the basis for induction of chronic stress. The experimental protocol is depicted in **Figure 1B**; animals were injected with TM every day for up to 15 days. Animals were sacrificed after either 5 or 15 days of injections, with the sacrifice taking place approximately 24h after the most recent dose (i.e., immediately before the next injection would have taken place). Animals were also sacrificed 8 hours after the first injection (D1-8h), to contrast the effects of chronic treatment with those of acute treatment using the same dose. After sacrifice, livers were harvested and analyzed for molecular and histological markers of ER stress.

Persistent underglycosylation of the ER-resident glycoprotein TRAP $\alpha$  at day 5 confirmed that TM remained pharmacologically active upon repeated dosing (**Figure 1C**). Yet despite these continued effects, the treatment led to initial alterations to liver histology that were progressively resolved. The predominant acute effect of TM on the liver, as revealed by hematoxylin and eosin staining, was the formation of intracellular vacuoles in hepatocytes (**Figure 1D**) that correspond to accumulated lipid droplets resulting from impaired lipid metabolism (Rutkowski *et al.*, 2008). The acute accumulation of lipid was confirmed by immunostaining with the lipid droplet marker adipose differentiation-related protein (ADRP). Other than these changes, there were few signs of gross liver damage such as necrosis or fibrosis (data not shown). Further, even this acute dysregulation of lipid metabolism progressively resolved despite

continued TM exposure, with liver histology and ADRP immunostaining returning to normal by 15 days (**Figure 1D, E**).

In order to test whether ER stress persisted in the chronic condition despite the apparent normalization of liver histology, we examined expression of BiP and CHOP proteins. Western blots confirmed an acute (D1-8h) increase in expression of both proteins. However, consistent with the effects of chronic stress on cultured cells (Rutkowski *et al.*, 2006), upregulation of the highly labile CHOP protein was lost (**Figure 1F**).

Taken together, these data indicate that chronic TM treatment caused persistent ER stress in the liver without permanently perturbing liver anatomy. They suggest that, as with cultured cells, hepatocytes *in vivo* are capable of adapting to long-term disruption of ER function if the stress is sufficiently mild. Thus, we used these conditions to investigate how the UPR is regulated during such adaptation.

#### *Chronic stress suppresses select UPR targets*

As the UPR is fundamentally a gene regulatory program, we examined the effects of chronic stress on UPR-dependent transcription. Despite *Chop* mRNA being upregulated by acute stress (**Figure 1A**), its expression returned to basal levels by 24 hours (D1-24h) and remained at similar levels at every subsequent time point (**Figure 2A**). This finding mirrored the behavior of CHOP protein (**Figure 1F**). Surprisingly, however, *Bip* mRNA levels—while elevated by acute stress (**Figure 1A**), were significantly diminished

by 24 hours and continued to diminish further through the first 5 days, and remaining suppressed thereafter (**Figure 2A**). Similar results were obtained using qRT-PCR primers bridging a separate pair of exons in *Bip* mRNA, demonstrating that this suppression reflected total *Bip* mRNA levels rather than alternate splicing (**Figure 2B**).

Using the D5-24h point as representative of chronic stress conditions, we next surveyed other UPR-regulated gene targets. While the expression of most mRNAs, like *Chop*, was not significantly different in the chronic condition, a subset displayed a similar downregulation to *Bip*. These included mRNAs encoding the transcription factor *Xbp1*, the ER-associated degradation factor *Herpud1*, and the ER chaperone *Grp94*. (**Figure 2C**). We also assessed the expression of metabolic genes that we and others have previously shown to be suppressed by ER stress in the liver (Rutkowski *et al.*, 2008; Yamamoto *et al.*, 2010; Arensdorf *et al.*, 2013a). While each of these was downregulated in the acute condition as expected (not shown), none was significantly suppressed in the chronic condition (**Figure 2D**). This finding provides evidence that the response of *Bip* and other mRNAs to chronic ER stress is mechanistically distinct from the pathways that suppress metabolic gene expression during acute stress.

*Chronic stress is associated with suppression of UPR-dependent transcriptional pathways*

The observation that all of the assessed UPR targets either were unregulated or were suppressed in the chronic condition suggested that, despite persistent upregulation of at least some proteins such as BiP, transcriptional regulation was a more dynamic process and might be suppressed during chronic stress, at least by the 24 hours that elapsed between each chronic stress time point and its most proximate dose of TM. One of the commonalities among the genes that were suppressed below basal levels is that each has been identified as a target of the ATF6 $\alpha$  pathway of the UPR (Yoshida *et al.*, 2001; Yamamoto *et al.*, 2004; Wu *et al.*, 2007). Thus, we hypothesized that the chronic condition would be accompanied by global suppression of UPR-dependent transcription to basal (i.e., unstressed) levels, but also by a further suppression of ATF6 $\alpha$  activity.

To test this hypothesis, we first assessed expression of the key UPR transcriptional regulators by immunoblot from liver nuclei. As expected, acute stress led to elevated expression of ATF4, XBP1<sub>spl</sub> and ATF6 $\alpha_{cl}$ ; however, all three were undetectable in the chronic condition (**Figure 3A**). This result was mirrored in a chromatin-immunoprecipitation (ChIP) experiment, which showed that acute stress enhanced the binding of ATF6 $\alpha$  to the *Bip* (locus: *Hspa5*) promoter (Yoshida *et al.*, 1998), but that this binding was lost in the chronic condition (**Figure 3B**). These ChIP data suggested that transcription of *Bip* was completely lost in the chronic condition, which was confirmed by ChIP directed against RNA Polymerase 2 (Pol2) at the *Hspa5* locus: As expected, Pol2 was recovered near the *Bip* transcriptional start site (-215 to +0), and this binding was unaffected by the presence or absence of ER stress (**Figure 3C**). This binding reflects Pol2 that is poised at the *Hspa5* promoter waiting to be

engaged during the transcriptional activation process (Muse *et al.*, 2007). In contrast, while Pol2 was abundantly recovered from the body of the *Hspa5* locus during acute stress (+2727 to +2906, which resides within an intron and reflects elongating polymerase), this binding was completely lost in the chronic condition (**Figure 3C**).

Taken together, these results demonstrate that ATF6 $\alpha$ -dependent transcription (and possibly XBP1- and ATF4-dependent transcription as well) is completely silenced in the chronic condition. However, for this inhibition of transcription to result in suppression of *Bip* mRNA expression compared to untreated animals, ATF6 $\alpha$  must contribute not only to stress-dependent transcription of *Bip* but also to the basal regulation of *Bip*. Confirming this prediction, we found that the basal expression of *Bip* in animals lacking ATF6 $\alpha$  was reduced by approximately 50 percent relative to wild-type animals, and that chronic stress then had no further effect on *Bip* expression (**Figure 3D**). Thus, loss of ATF6 $\alpha$  alone was sufficient to mimic chronic stress treatment. From these data, we conclude that at least the ATF6 $\alpha$  pathway of the UPR is engaged in the liver absent exogenous stress, and that even this basal component can be inhibited upon chronic stress.

*Chronic stress is marked by cycles of activation and deactivation that suppress UPR-dependent transcription but maintain RIDD*

To this point, our data establish that under conditions of chronic stress, UPR-dependent transcription is attenuated, including, apparently, the contribution of ATF6 $\alpha$  to basal *Bip*



expression. This attenuation could come about in either of two ways. One possibility is that some fundamental feature of chronic stress renders the UPR increasingly refractory. This means that after 5 days of activation by successive bouts of stress the UPR would no longer be responsive. This is a “preconditioning” model, and would be similar to behavior that we observed in MEFs *in vitro* upon repeated exposure to stress (Rutkowski *et al.*, 2006). The other possibility is an “augmented deactivation” model in which the UPR is activated in full or nearly so upon each exposure to stress, but the temporal dynamics of its activation and resolution become progressively altered. In other words, the question is whether chronic stress mutes the activation of the UPR (*preconditioning*) or enhances its deactivation (*augmented deactivation*).

To distinguish between these possibilities, we examined the temporal response of the UPR in animals exposed to either the first dose of TM or the fifth dose (**Figure 4A**). Rather than following the production of UPR-regulated transcription factors as in **Figure 3**, we instead monitored activation of the UPR sensor IRE1 $\alpha$ , which serves as a direct, robust, and sensitive readout for the capacity of the UPR to be activated. IRE1 $\alpha$  was monitored using *Xbp1* mRNA splicing (**Figure 4B**). This experiment demonstrated that the UPR remained essentially as stress-responsive on the fifth day as on the first; splicing of *Xbp1* 8 hours after the first injection and 8 hours after the fifth were induced to comparable levels. Yet the *deactivation* of the UPR, or at least the *Xbp1* splicing activity of IRE1 $\alpha$ , proceeded more rapidly on day 5 than on day 1; substantial *Xbp1* splicing was seen 14 hours after the first injection but not 14 hours after the fifth. We also monitored *Bip* mRNA expression over the same time course, and found that its

expression mirrored the pattern of *Xbp1* splicing—namely, that *BiP* expression was well-induced after both treatments (albeit about two-fold less robustly in the chronic condition), but that its attenuation proceeded more rapidly in the chronic condition (**Figure 4C**).

These data reveal two features of the response to chronic stress: First, they show that, even upon repeated activation, the UPR remains capable of recognizing and responding to ER stress. And second, they show that the response to chronic stress in this experimental system appears to fundamentally involve augmented versions of the same mechanisms that deactivate the UPR upon a single exposure to stress. Thus, the chronic treatment opens a window into the mechanisms of UPR deactivation, about which relatively little is known since ER stress is usually studied in the context of stresses sufficiently severe as to kill cells.

These experiments also yielded an additional insight, which was that the rapid loss of *Bip* mRNA by the fifth day might not be accounted for solely by the loss of *Bip* transcription. *Bip* mRNA levels decreased more than 30-fold between 8 hours and 24 hours on the fifth day, for a half-life of approximately 3 hours (**Figure 4C**). However, by monitoring *Bip* expression after treatment of primary hepatocytes with the transcription inhibitor Actinomycin D, we measured *Bip* mRNA half-life after treatment with TM at 8.2 hours (**Figure 4D**), consistent with our previous measurement in MEFs (Rutkowski *et al.*, 2006). The simplest explanation for these results is that deactivation of the UPR is accompanied by stimulated degradation of *Bip* mRNA, for even the loss of *Bip* that

occurs on the first day of treatment (**Figure 4C**) is too rapid to be accounted for by inhibition of transcription alone.

An obvious candidate for stimulated degradation of *Bip* mRNA would be Regulated IRE1-dependent decay (RIDD), which is the process by which activated IRE1 directly degrades ER-associated mRNAs (Hollien *et al.*, 2009). This process is thought to be counter-adaptive, facilitating cell death during severe ER stress (Han *et al.*, 2009; Upton *et al.*, 2012). However, it has also been implicated in metabolic regulation in the liver (Cretenet *et al.*, 2010; So *et al.*, 2012), implying that perhaps its function is more nuanced. *Bip*, *Grp94*, and *Herpud1* mRNAs would be expected to localize to the ER by virtue of encoding proteins bearing ER targeting signals. *Xbp1* mRNA has also been shown to localize to the ER through a pseudo-signal sequence in the XBP1 protein (Yanagitani *et al.*, 2009). *Xbp1* is obviously a target of the IRE1 $\alpha$  nuclease, while *Bip* at least has also been proposed to be a RIDD target, though with unclear functional significance (Han *et al.*, 2009).

To test whether RIDD was active in the chronic stress condition, we assessed the expression of the well-validated RIDD target *Bloc1s1* (aka *Blos1*). Among putative RIDD targets, only *Bloc1s1* has been documented in multiple reports, and in highly diverse cell types (Bright *et al.*, 2015). We confirmed that *Bloc1s1* is a *bona fide* RIDD target in MEFs lacking IRE1 $\alpha$  (**Figure 4E**). As expected, *Bloc1s1* expression was reduced by acute TM treatment (**Figure 4F**). Furthermore, there remained a more modest but still significant reduction in *Bloc1s1* expression in the chronic condition (**Figure 4F**). This result was mirrored in the expression of *, which we found to be a potential RIDD*

target in the liver based on microarray data from wild-type and liver-specific *Ire1α*- mice treated with TM (Zhang *et al.*, 2011). This behavior is in contrast to genes such as *Chop*, *Wars*, etc., that are transcriptionally induced by acute ER stress, and which did not remain induced in the chronic condition (**Figure 2C**), as well as to metabolic genes that are transcriptionally repressed by acute ER stress, which do not remain repressed in the chronic condition (**Figure 2D**). Computational modeling suggests that mRNAs whose expression is regulated by stimulated degradation should return to basal expression levels much more rapidly than those whose regulation is transcriptional, when both mechanisms are deactivated (Arendsdorf *et al.*, 2013b). Thus, this persistence of *Bloc1s1* and *Fn1* suppression suggests that, in contrast to the pathways of transcriptional regulation, RIDD activity persists through the cycles of UPR activation and deactivation that characterize the chronic stress state, even while the *Xbp1* splicing activity of IRE1 $\alpha$  is attenuated.

#### *Overexpression of BiP is sufficient to suppress Bip and Grp94 mRNA*

Our results to this point suggest that the downregulation of select mRNAs seen in the chronic condition is in fact an augmentation of the deactivation of the UPR that occurs as stress is resolved—essentially, that with each successive exposure to stress, the UPR becomes more efficient at deactivation, even to the point of overshooting, while still retaining its activation capacity. The mechanisms of deactivation, however, are poorly understood. One pathway by which the UPR is deactivated is upregulation of

BiP, which turns off the response in two ways: by improving ER protein folding (in concert with the many other factors regulated by the UPR); and by directly binding to the UPR stress sensors (IRE1 $\alpha$ , ATF6 $\alpha$ , and PERK) and repressing their activation (Bertolotti *et al.*, 2000; Shen *et al.*, 2002).

In the chronic condition, *Bip* mRNA was suppressed despite ongoing upregulation of BiP protein (**Figure 1F**); the same was true for GRP94 (not shown). Given the repeated cycles of activation that characterize the chronic response (**Figure 4**), it is perhaps unsurprising that BiP accumulates to the extent that it does; we have previously measured the half-life of BiP protein in MEFs at approximately 2 days (Rutkowski *et al.*, 2006), and it appears to also be long-lived in hepatocytes (not shown). This persistent BiP protein expression thus provides a potential means by which UPR deactivation could be accelerated.

To test this hypothesis, we ectopically overexpressed BiP protein in the liver using recombinant adenovirus (*ad-BiP*, aka *ad-Grp78*) (Young *et al.*, 2012). After injection of *ad-BiP*, we observed a significant increase in BiP protein expression compared to *ad-GFP* expressing animals (**Figure 5A**). qRT-PCR confirmed the efficacy of exogenous *Bip* overexpression (**Figure 5B**). Using primers that detect the 5' UTR of *Bip* mRNA (and thus amplify only endogenous *Bip* and not exogenous), we found that, like chronic stress, BiP protein overexpression also suppressed *Bip* mRNA expression (**Figure 5C**). Similar results were obtained for *Grp94*, while overexpression had no effect on *Chop* expression (**Figure 5C**). Surprisingly, *Bloc1s1* expression was also suppressed under these conditions, again mirroring the chronic condition (**Figure 5D**).

This finding hints that the apparent persistence of RIDD in the chronic condition (**Figure 4G**) might reflect a unique sustainment of that activity of IRE1 $\alpha$  by BiP during recovery from stress when the transcriptional limbs of the UPR are suppressed.

The effects of BiP overexpression on *Bip* and *Grp94* mRNA and RIDD could be due to either enhanced protein folding in the ER or due to direct effects of BiP on the UPR sensors independent of the protein folding capacity. We found that treating mice with the pharmacological chaperone TUDCA (Özcan *et al.*, 2006)—which reduced upregulation of ER stress markers by TM approximately 2-fold—had no effect on its own on any UPR gene tested (**Figure 5E**). These data show that improved ER protein folding capacity was not sufficient to suppress *Bip* expression. While they do not completely rule out the possibility that improved ER protein folding ultimately drives *Bip* suppression in the chronic condition, they nonetheless lead us to favor a model whereby BiP directly modulates the activities of at least ATF6 $\alpha$  and IRE1 $\alpha$ .

*Suppression of Bip expression and activation of RIDD are mirrored in the livers of genetically obese animals*

To what extent are the regulatory events described here relevant to physiological chronic stresses? Repeated dosing with TM, while effective as a tool for inducing ER stress, is nonetheless doubtless much more robust and focal a stress than anything commonly encountered physiologically. However, the cyclic nature of the stimulus—bouts of stress followed by periods of recovery—might to some extent mirror the stress

caused by metabolic flux, which is tied to feeding and fasting cycles and is thus by its nature cyclic. The notion that overnutrition—i.e., consumption of too much food per meal and/or too many meals—might represent a chronic ER stress was first suggested in 2004, in seminal work demonstrating that ER stress was observed in the livers of obese mice, and was tied to hepatic insulin resistance (Özcan *et al.*, 2004). Thus, we considered the possibility that feeding is capable of eliciting the same changes in gene regulation as seen in the TM-induced chronic condition.

Consistent with previous reports (Oyadomari *et al.*, 2008; Pfaffenbach *et al.*, 2010), we found that feeding elicited ER stress in mouse livers (**Figure 6A**). Interestingly, this effect was much more robust for some targets (*Bip*, *Grp94*, and *Xbp1*) than others; in fact, targets of the PERK pathway (*Chop*, *Gadd34*, and *Wars*) were not upregulated to a statistically significant extent under these conditions. Feeding also elicited splicing of *Xbp1* mRNA as measured by qRT-PCR using primers that preferentially amplify only the spliced form (*Xbp1(s)*, **Figure 6A**), albeit to a very modest extent (once the change in total *Xbp1* levels is accounted for). While it has been proposed that a high fat diet is intrinsically stress-inducing (Özcan *et al.*, 2004), at least in this instance we found no difference between the level of stress induced by diets containing either high fat or no fat (**Figure 6A**). This result indicates that nutrient intake itself elicits ER stress, and is consistent with the idea that the stress is driven by increased anabolism (Özcan *et al.*, 2008) rather than fat *per se*. As we speculated, this stress is modest compared to that induced by TM, for which most UPR targets were

induced to an extent that was an order of magnitude or more greater than feeding (**Figure 6B**).

If feeding represents an ER stress, then repeated feeding should represent a chronic stress, particularly if it outpaces the ability of the organelle to compensate. Thus, we examined gene expression in *ob/ob* or *db/db* mice, which are obese due to mutations in leptin or the leptin receptor, respectively, that compromise appetite control and lead to overfeeding (Campfield *et al.*, 1995; Halaas *et al.*, 1995; Pelleymounter *et al.*, 1995; Chen *et al.*, 1996; Lee *et al.*, 1996). We observed a similar pattern of gene regulation in these animals as in animals treated with chronic TM; *Bip*, *Grp94*, and *Xbp1* were all significantly suppressed (**Figure 6C**), while other UPR targets were not suppressed (and, indeed, appeared to be upregulated; **Figure 6D**). In addition, again mirroring the results seen in TM-treated animals, expression of *Bloc1s1* was reduced in *db/db* mice and potentially in *ob/ob* mice as well, and *Fn1* was strongly suppressed in both (**Figure 6E**). These data support the idea that the experimental induction of chronic ER stress is a useful tool for understanding how gene regulatory patterns are altered by chronic physiological stresses.



## Discussion

In this paper, we have described the first, to our knowledge, experimental reconstitution of chronic, tractable ER stress in a mammal *in vivo*. This work builds upon previous efforts to recreate chronic ER stress in fish larvae (Cinaroglu *et al.*, 2011), and to elicit chronic ER stress in mammals by overexpression of misfolded ER client proteins or deletion of ER chaperones (e.g., (Ji *et al.*, 2011; Zode *et al.*, 2011; Kawasaki *et al.*, 2015)). We have used this system as a tool to probe how UPR signaling becomes altered during persistent and/or repeated activation. Our investigation has several novel implications for the mechanisms of UPR signaling.

The data presented here lead us to propose a working model to account for the altered expression of *Bip* and other UPR transcriptional targets during chronic stress (**Figure 7**). In the basal (i.e., nominally “unstressed”) state, activation of ATF6 $\alpha$  contributes to the expression of *Bip* mRNA. We arrive at this conclusion because expression of *Bip* was diminished in the absence of ATF6 $\alpha$  even without an exogenous stress (**Figure 3D**). This finding implies that normal physiological function in the liver entails periods of UPR activation—perhaps not surprisingly, given that feeding itself activates the UPR (**Figure 6A**). BiP is one of the most abundant proteins in the ER lumen (Gething, 1999), and other non-stress-dependent mechanisms contribute to its basal regulation as well (Resendez *et al.*, 1988). Upon exposure to a conventional ER stress, all three limbs of the UPR are activated (Rutkowski *et al.*, 2006), leading to robust production of stress-specific target transcripts such as *Chop*, as well as

augmentation of transcripts encoding ER chaperones, such as *Bip* and *Grp94*. The attendant improvement of ER protein folding then presents a problem for the cell: how to avoid overproduction of UPR targets. As the UPR stress-sensing molecules become deactivated, naturally labile factors such as CHOP (both mRNA and protein) are readily lost (Rutkowski *et al.*, 2006). However, ER chaperones such as BiP and GRP94 are long-lived at both the protein and mRNA levels (Rutkowski *et al.*, 2006), and continued overproduction of these proteins would presumably greatly tax cellular resources and potentially constitute their own burden on the organelle. Thus, BiP overexpression appears to initiate a negative feedback loop, both suppressing UPR activity (including the basal activity of ATF6 $\alpha$ ) and also stimulating the degradation of its own mRNA. In the context of incidental exposure to stress, or of the low-level stresses that occur during normal physiological function, we presume that this depression of *Bip* mRNA levels is transient. However, during repeated stress, we propose that it constitutes a new quasi-stable setpoint for UPR transcriptional regulation.

One of the founding observations of the UPR field was that activation of the ER stress sensing molecules required their dissociation from BiP in both yeast and mammals (Bertolotti *et al.*, 2000; Shen *et al.*, 2002). Originally, the purpose attributed to BiP binding was to hold the stress sensors in a quiescent state and so to play a role in UPR activation. However, the suggestion that at least yeast Ire1p can be activated by direct binding to unfolded proteins (Kimata *et al.*, 2004; Gardner and Walter, 2011; Gardner *et al.*, 2013) has cast doubt on this model. Our data raise the possibility that perhaps the role of BiP binding is to instead modulate UPR *deactivation*.

The objective of this work from the outset was to develop an experimental system for eliciting chronic ER stress *specifically*, in order to be able to determine how the regulation and output of the response changed under such conditions and so identify fingerprints of chronic ER stress associated with disease states. Toward that end, the strikingly similar phenotype in *ob/ob* and *db/db* mice vouches for this approach. One difference between the chronic condition on one hand and the steady-state in obese mice on the other is that the latter do not appear to express elevated BiP protein levels (not shown), which at face value seems at odds with the idea that elevated BiP protein is needed to both suppress ATF6 $\alpha$  and activate or perpetuate RIDD. However, as we have demonstrated, the magnitude of ER stress elicited by feeding is considerably lower than that elicited by tunicamycin (**Figure 6**; also compare **Figure 6A** with **Figure 4C**), yet also much more repetitive than the once-daily TM challenge. It is plausible that the less robust but more constant stimulus of overfeeding results in modest alterations in expression of BiP protein that have little effect on *Bip* mRNA over the course of meals or days but great effect over the course of months—essentially that small increases in BiP protein levels could produce small decreases in BiP mRNA expression that accumulate over time. It is possible that further moderating the dose of TM and lengthening its extent (from days to weeks/months) would more closely mimic the phenotype observed in obese animals, although this would be experimentally cumbersome. Ultimately, the clearest way to test whether the same mechanism is at work might be to intercross obese animals with *Atf6 $\alpha$ -/-* animals; as when given repeated TM injections, these animals should have basally suppressed *Bip* mRNA

expression even at an early age, but then there should be no further suppression as the animals age and become obese. Even if the mechanism turns out to be entirely distinct, the description here of suppressed expression of *Bip*, *Grp94*, and *Xbp1* and apparently elevated RIDD activity in these animals has potential implications for their ability to maintain ongoing ER homeostasis. It is conceivable that an altered UPR “setpoint” with reduced expression of *Bip* and other UPR mRNA targets could render the animals more sensitive to ER stress-induced cell death and exacerbate the hepatic inflammation associated with obesity (Gregor and Hotamisligil, 2011).

A surprising conclusion from this work is that RIDD appears to remain active in the chronic condition, even as UPR-dependent transcriptional signaling is shut off. Admittedly, conclusively demonstrating RIDD activity *in vivo* is challenging; here we have relied on repression of the well-documented RIDD target *Bloc1s1* as the primary readout for RIDD activity. *Bloc1s1* expression was repressed in the chronic condition (**Figure 4G**), upon BiP overexpression (**Figure 5D**), and in *db/db* animals (**Figure 6E**). Phos-tag immunoblotting showed substantial phosphorylation of IRE1 $\alpha$  only in animals treated with a high acute dose of TM, and antibodies purported to be specific for phospho-IRE1 did not produce bands absent in *Ire1 $\alpha$* <sup>-/-</sup> cells in control experiments (not shown). These limitations made it impossible to directly test whether IRE1 $\alpha$  remains phosphorylated in the chronic condition. In addition, there is as yet no functional assay for confirming that RIDD is active *in vivo*. Rather, substrates are generally identified as putative RIDD targets based on an *in vitro* assay using purified IRE1 $\alpha$  (Hollien and Weissman, 2006; Hollien *et al.*, 2009). Then, their RIDD dependence is confirmed by

their suppression during ER stress in an IRE1 $\alpha$ -dependent XBP1-independent manner. However, *Bip* and *Grp94* are both also transcriptionally upregulated by XBP1 (Lee *et al.*, 2003), which would likely confound analysis of their regulation in *Ire1 $\alpha$* <sup>-/-</sup> animals. In any case, our data hint at a previously unappreciated role for RIDD, which has generally been considered an anti-adaptive signaling mechanism to this point (Han *et al.*, 2009; Lerner *et al.*, 2012; Upton *et al.*, 2012; Maurel *et al.*, 2014). The purpose of the clearance of ER-resident proteins might not so much be to neuter the organelle and hasten its dysfunction during severe stress (Maurel *et al.*, 2014) as to help to turn the response off once stress has been overcome. Such a role could help explain the previously puzzling finding that *Bip* is a potential RIDD target (Han *et al.*, 2009).

Assuming RIDD is indeed active during chronic stress, our data provide further evidence that the *Xbp1* splicing and RIDD activities of IRE1 $\alpha$  can be dissociated (Lin *et al.*, 2007; Han *et al.*, 2008). They raise the possibility that this dissociation occurs not necessarily to separate adaptive from apoptotic outputs so much as to separate activation from deactivation. Given that most stresses encountered by most cells most of the time are likely to be mild and transient—such as that encountered by feeding—the death-accelerating function of RIDD might simply be a byproduct of a normal physiological role in restoring the UPR rheostat. Indeed, a parallel can be drawn with the UPR-regulated transcription factor CHOP which, though it clearly promotes cell death during severe stress (Zinszner *et al.*, 1998) also might promote normal cellular function during milder stress both by potentiating the dephosphorylation of eIF2 $\alpha$

(Marciniak *et al.*, 2004) and by regulating lipid metabolism (Tyra *et al.*, 2012; Chikka *et al.*, 2013) toward the ultimate improvement of ER function.

The approach we took to experimentally reconstituting chronic ER stress *in vivo* was conceptually analogous to our earlier reconstitution of chronic stress *in vitro* in MEFs (Rutkowski *et al.*, 2006). However, neither MEFs nor even cultured hepatocytes showed the same suppression of *Bip* expression as seen *in vivo*. This discrepancy points to the existence of other as yet unappreciated factors that influence UPR output in the liver. Indeed, it is now becoming clear that, overlaid atop the structural framework of the canonical UPR lie modulatory pathways for altering UPR sensitivity and output, with potential implications for signaling during chronic stress. These include posttranslational modifications either of the stress sensors—such as S-nitrosylation of IRE1 $\alpha$  (Yang *et al.*, 2015)—or of ER chaperones, such as ADP ribosylation (Chambers *et al.*, 2012) or AMPylation (Preissler *et al.*, 2015) of BiP. It will be interesting to test whether any of these modifications is active during the chronic condition.

Finally, our results underscore the remarkable capacity of the UPR to adapt to chronic stress. While the severe experimental stresses that lead to massive cell death and organ dysfunction have proven useful in elucidating the signaling capabilities of the UPR when activated to its maximum, they yield little about the ebb and flow of the response at it is most likely to be activated in physiological scenarios. We hope that our approach will stimulate further efforts to more closely mimic physiological stresses *in vivo*, as these will be essential in linking chronic ER stress to human disease.

## Materials and Methods

### *Animal Experiments*

All protocols for animal use were reviewed and approved by the University Committee on Use and Care of Animals at the University of Iowa. Animals were fed standard rodent chow and housed in a controlled environment with 12h light and dark cycles. Animals used were of both genders unless otherwise noted, with control and experimental groups having similar composition. Animals were fasted for 4h prior to sacrifice, which was carried out during the lights-on period. *Atf6 $\alpha$ -/-* (Wu *et al.*, 2007) animals have been backcrossed into the *C57BL/6J* strain for >10 generations. For chronic TM (EMD Millipore) treatment, 8 to 12 week old *C57BL/6J* or *Atf6 $\alpha$ -/-* mice were injected once per day (~1 hour after lights-on) intraperitoneally with vehicle or the indicated dose of Tunicamycin dissolved in PBS and were sacrificed at various timepoints after last injection. For TUDCA (EMD Millipore) treatment, animals were injected IP with vehicle or 500 mg/kg TUDCA in PBS once daily, 1 hour after lights-on for 10 days prior to sacrifice. 8 hours prior to sacrifice (3 hours after lights-on), animals were injected with TM or vehicle. For high fat/no fat feeding, animals were habituated for 5d to a standard defined diet (D12450B, Research Diets), fasted 20h, and then either injected with 1 mg/kg TM for 4h or provided access to a high fat diet (D12451, 45% fat) or a no-fat diet (D10062804, 0% fat) for 4h. *ob/ob* and *db/db* samples were taken from 5 month-old female mice.

Harvested liver tissue pieces were either frozen immediately for RNA or protein analysis, fixed in formalin (for IHC), processed for nuclear isolation, or minced and fixed in formaldehyde (for ChIP). Nuclei were isolated as described (Rutkowski *et al.*, 2008). For histological analysis, formalin-fixed tissues were embedded in paraffin, sectioned, and stained with hematoxylin and eosin, or subjected to IHC to detect ADRP as described (Chikka *et al.*, 2013). Antibodies used for immunoblot were as in (Chikka *et al.*, 2013), and as follows: ATF4 (sc200, Santa Cruz); XBP1 (sc7160, Santa Cruz); ATF6 $\alpha$  (non-commercial antibody). Antibodies were generally incubated on blots in TBS-Tween + 5% milk at room temperature for 1 hour except for ATF6 $\alpha$  antibody, which was incubated in PBS-Tween + milk at 4°C overnight.

### *Cell Experiments*

MEFs were harvested as described previously (Lee *et al.*, 2002) from *Ire1 $\alpha$ <sup>-/-</sup>* or *Ire1 $\alpha$ <sup>+/+</sup>* mice. Isolation of primary hepatocytes was as in (Fan *et al.*, 2004) with minor modifications. Hepatocytes were isolated from *C57BL/6J* mice. Mice were anesthetized with isoflurane. The liver was perfused through the portal vein first with Perfusion Buffer Solution and then with Liver Digest Medium. Formulations were as follows: Liver Perfusion Media: HBSS, no calcium, no magnesium, no phenol red (Life Technologies), 0.5mM EGTA, 0.5mM EDTA, 25mM HEPES, Penicillin-Streptomycin (10,000 U/mL) (Life Technologies) and 0.2% BSA (Research Products International); Liver Digest Media (50mL for 25g mouse): HBSS, calcium, magnesium, no phenol red (Life Technologies), 0.25mM HEPES, Penicillin-Streptomycin (10,000 U/mL) (Life



Technologies), 3.6mg Trypsin Inhibitor (Sigma), 28mg Collagenase Type IV (Life Technologies) added fresh. Digest flow rates were 5 mL/min for 5 minutes for perfusion and 10 min for digest. The liver was then quickly dispersed and filtered through a sterile 100  $\mu$ m mesh. Hepatocyte suspensions were then centrifuged at 50x g for 3 minutes and resuspended to a density of  $5 \times 10^6$  cells/ml in DMEM. Viable hepatocytes in the pellet were washed three times and then plated on collagen-coated tissue culture plates in DMEM with 10% calf serum and 100  $\mu$ g/ml penicillin and streptomycin. After overnight culture, the medium was replaced with F-12 medium containing insulin (10  $\mu$ g/ml), dexamethasone (67 ng/ml), triiodothyronine (67.3 ng/ml), penicillin (100 units/ml), and streptomycin (0.1 mg/ml). Primary hepatocytes were treated with 5  $\mu$ g/mL of TM for 4h before addition of ActinomycinD (ActD; Sigma) to 5  $\mu$ g/mL. Cells were collected in triplicate 15 min after addition (0 hour), 2h 15m, and 4h 15m after treatment.

### *Adenovirus Experiments*

*Ad-Bip* and was created as described (Young *et al.*, 2012) and amplified by the University of Iowa Gene Transfer Vector Core. Control virus expressing GFP only (*Ad-Gfp*) was also obtained from the Vector Core.  $3 \times 10^9$  pfu/mouse were administered through tail vein injections for hepatic expression. Experiments were performed 5 days later.

### *Molecular Analysis*

RNA and protein analyses were performed as described (Rutkowski *et al.*, 2006).

Immunoblots were imaged using the ChemiDoc-It imaging system (UVP, LLC, Upland, CA) with on-chip integration and empirically derived exposure settings. Membranes were sliced into appropriate molecular weight ranges for blotting; membranes were never stripped and reprobed. Images were processed using Adobe Photoshop. Black hairlines are solely to aid in visual assessment. All contrast adjustments were performed uniformly. Primer sequences and methods utilized for real-time PCR analysis have been published previously (Rutkowski *et al.*, 2006; Rutkowski *et al.*, 2008; Arensdorf *et al.*, 2013a). *Xbp1* RT-PCR was as described (Tyra *et al.*, 2012). Additional primers are described here: *Xbp1(s)*: Fwd GAGTCCGCAGCAGGTG, Rev GTGTCAGAGTCCATGGGA; genomic Bip Primer (5' UTR of Bip gene) Fwd TAAGACTCCTGCCTGACTGC, Rev GGAATAGGTGGTCCCCAAG; ChIP primers: *Bip* Promoter (-215 to +8 bp) Fwd CATTGGTGGCCGTTAAGAATGACCAG, Rev AGTATCGAGCGCGCCGTCGC; *Bip* Int7 (+2727 to +2906) Fwd GGGAGGACTGTTGCTTTAGG, Rev TGAATGAACTCTTGCCATCTTC.

### *Chromatin Immunoprecipitation*

ChIP was performed as in (Arensdorf and Rutkowski, 2013; Chikka *et al.*, 2013) with minor modifications. Formaldehyde-fixed liver tissues were weighed out after being quenched with 1.5M Tris-HCl and pulverized in a metal mortar and pestle. Samples were sonicated using a Covaris E220 sonicator. Chromatin was immunoprecipitated using ATF6 $\alpha$  (H-280 X, Santa Cruz) or Pol II (N-20 X, Santa Cruz) antibodies or non-

specific IgG (12–370, Millipore) overnight at 4°C. DNA was purified using a standard phenol/chloroform extraction protocol. Samples were then analyzed by quantitative real-time PCR with an annealing temperature of 58°C.

### *Statistical Analysis*

Groups were compared by one-way ANOVA. Tukey's Post-Hoc analysis was used when comparing multiple conditions for the same readout.

### **Acknowledgments**

We thank R. Davisson (Cornell) for the *Ad-Bip* virus (aka AdGRP78), R. Kaufman (Sanford Burnham) for *Atf6 $\alpha$ <sup>-/-</sup>* mice, and R. Hegde (MRC, Cambridge) for TRAP $\alpha$  antibody. At the University of Iowa, we thank A. Peluzzo and J. Zabner for *ob/ob* and *db/db* mice, F. Jo and C. Sigmund for advice on TUDCA experiments; K. Nillson and D. Price for advice on ChIP; and L. Yang for stimulating discussions. This work was funded by NIH grant GM115424 to D.T.R. and by funds from the University of Iowa Department of Anatomy and Cell Biology, the Carver College of Medicine, and the Office of the Vice President for Research. J. A. G. was supported by NIH training grant GM067795 as well as funds from the University of Iowa Office of Cultural Affairs and Diversity Initiatives and the Graduate College.

### **Author Contributions**

D.T.R. and J.A.G. conceived and designed the experiments, analyzed the data, and wrote the paper. J.A.G. performed most of the experiments. D.T.R. performed some of the experiments.

## Figure Legends

### Figure 1. Mice adapt to repeated exposure to TM despite persistent stress.

**(A)** Livers from wild-type mice collected 8h after injection with the indicated concentrations of TM (in mg/kg) were probed by qRT-PCR for expression of *Bip* and *Chop*. Data represent means  $\pm$  S.E.M. n=3 animals/group. Significance was calculated for treatment by one-way ANOVA. Here and elsewhere, \*\*\*,  $p < 0.001$ ; \*\*,  $p < 0.01$ ; \*,  $p < 0.05$ ; NS = not significant **(B)** Chronic stress treatment schematic. Mice were weighed and then injected daily with 0.025 mg/kg TM (red arrows); liver samples were collected at the indicated times (blue arrows) for downstream analysis. The naming convention is as follows: “D” indicates the number of daily injections received while “h” indicates the time of tissue collection after the last injection. **(C)** Samples were harvested at the indicated times and protein lysates were probed by immunoblot to detect the ER-resident glycoprotein TRAP $\alpha$  and its singly (+1 CHO) and doubly (+2 CHO) N-glycosylated forms. Each lane represents a single mouse. Here and elsewhere, not treated animals (NT) received injections of vehicle at the same times that D5-24h mice received TM. Calnexin was used as a loading control. **(D)** Liver sections were collected, fixed and stained by H&E at the indicated times. Representative images using the 20x objective are shown above, while the black box indicates zoomed-in area. Note the cytoplasmic vacuolization in the zoomed image. **(E)** Formalin-fixed liver samples were immunostained to detect the lipid droplet marker protein ADRP. **(F)** Protein lysates

were isolated as in (C) and probed for expression of BiP and CHOP. Calnexin was used as the loading control.

## **Figure 2. Chronic stress suppresses a subset of UPR target genes.**

**(A)** Mice were injected with 0.025 mg/kg TM daily for up to 18 days, and livers were collected 24h after the last injection as indicated. Expression of *Bip* and *Chop* was measured by qRT-PCR. Expression is given relative to non-treated control mice. Data for all chronic stress experiments is shown on a  $\log_2$  scale. n=2-3 animals/group **(B)** Expression of *Bip* using an alternate primer pair spanning a different exon/intron junction confirms results from (A). **(C)** qRT-PCR of a group of UPR target genes from animals treated with vehicle or TM for 5d. n=8 animals/group. **(D)** Expression of the indicated metabolic genes was determined by qRT-PCR from an experiment similar to (C), except injections were performed for 7d. n=4 animals/group.

## **Figure 3. Chronic stress silences ATF6 $\alpha$ -dependent transcription.**

**(A)** After treatment of mice with 0.025 mg/kg TM for either 8h or 5d, nuclei were isolated from liver lysates and probed with antibodies against ATF4, XBP1, or ATF6 $\alpha$ . Specificity of all antibodies was confirmed by immunoblot from knockout or overexpression cells or liver lysates (not shown). The loading control for ATF4 and XBP1 blots was PARP. The loading control for the ATF6 $\alpha$  immunoblot is a nonspecific background band (\*). **(B)** After TM treatment as in (A), control Ig or antibodies against ATF6 $\alpha$  were used to immunopurify the *Bip/Hspa5* promoter region, which was then amplified by qPCR using primers directed against two overlapping regions in the promoter containing the ER

stress elements (ERSEs) or a control sequence. Number is given relative to the transcriptional start site. n=4 animals/group **(C)** Same as (B), except ChIP was performed using antibodies against RNA Polymerase 2. The -215 to +8 regions detects poised polymerase and so does not change, while the +2727 to +2906 region is within a downstream intron and detects elongating Pol2. **(D)** Wild-type or *Atf6 $\alpha$* <sup>-/-</sup> mice were treated with 0.025 mg/kg TM or vehicle for 5d. qRT-PCR expression of *Bip* in the liver was assessed using both primer sets. *Bip* expression was suppressed to comparable levels by either chronic stress or deletion of *Atf6 $\alpha$* , but chronic stress had no effect in *Atf6 $\alpha$* <sup>-/-</sup> animals. n=3-5 animals/group

**Figure 4. Accelerated degradation diminishes *Bip* mRNA levels during chronic stress.**

**(A)** Schematic showing treatment protocol; livers were harvested 8, 14, 20, or 24h after either the first TM injection or the fifth. **(B)** Conventional RT-PCR was used to distinguish spliced (spl) from unspliced (us) *Xbp1* mRNA in samples treated as in (A). Image is inverted black-to-white for greater visual clarity. **(C)** *Bip* mRNA expression was assessed by qRT-PCR from samples treated as in (A). **(D)** Primary hepatocytes were isolated from a wild-type mouse, and treated with TM in the presence or absence of actinomycin D (ActD) to inhibit transcription as described in Materials and Methods. *Bip* half-life was calculated from these data. n=3 plates/group **(E)** Wild-type or *Ire1 $\alpha$* <sup>-/-</sup> mouse embryonic fibroblasts (MEFs) were treated with TM for 8h and expression of the RIDD target *Bloc1s1* was determined by qRT-PCR. n=3 plates/group **(F)** Animals were

treated for 8h or 5d with 0.025 mg/kg TM as in Figure 1B. Expression of *Bloc1s1* and *Fn1* was determined by qRT-PCR. n=4 animals/group

**Figure 5. Overexpression of exogenous BiP is sufficient to repress endogenous *Bip* expression.**

**(A)** Animals were injected with recombinant adenovirus expressing either GFP or BiP. 5d after injection, mice were sacrificed and BiP was probed by immunoblot. Loading control was calnexin. **(B)** Both primer sets detected elevated *Bip* expression in *ad-BiP* mice, which is attributable to the contribution of the exogenous *Bip*. **(C, D)** Expression of endogenous *Bip* from the genomic locus (*gen-Bip*), *Grp94*, or *Chop* (C) or *Bloc1s1* (D) was assessed in *ad-GFP* and *ad-BiP* animals by qRT-PCR. n=6-8 animals/group **(E)** Wild-type animals were treated for 10d with 500 mg/kg TUDCA, and then for 8h with 0.025 mg/kg TM, and expression of the indicated genes was detected by qRT-PCR. TUDCA was sufficient to reduce stress-induced expression of these genes approximately two-fold or more, but not to suppress basal *Bip* expression. n=3-6 animals/group

**Figure 6. Genetically-induced obesity phenocopies chronic stress.**

**(A)** Wild-type animals were fasted overnight, and then provided food containing either 45% fat or no fat for 4h. Expression of the indicated genes was assessed by qRT-PCR. n=3 animals/group **(B)** Wild-type animals were treated with 1 mg/kg TM for 4h, and the same genes as in (A) were detected by qRT-PCR. #; p<0.1. n=3 animals/group **(C-E)**



Livers from 5 month-old female *ob/ob* or *db/db* mice or age-matched wild-type mice were probed for expression of genes that were suppressed by chronic stress (C) or not-suppressed (D), or of the RIDD target *Bloc1s1* and the putative RIDD target *Fn1* (E).

n=4 animals/group

**Figure 7. Model for UPR dynamics during chronic stress.**

See Discussion for details.

## References

- Arensdorf, A.M., DeZwaan McCabe, D., Kaufman, R.J., and Rutkowski, D.T. (2013a). Temporal clustering of gene expression links the metabolic transcription factor HNF4 $\alpha$  to the ER stress-dependent gene regulatory network. *Front Genet* 4, 188.
- Arensdorf, A.M., Diedrichs, D., and Rutkowski, D.T. (2013b). Regulation of the transcriptome by ER stress: non-canonical mechanisms and physiological consequences. *Front Genet* 4, 256.
- Arensdorf, A.M., and Rutkowski, D.T. (2013). Endoplasmic reticulum stress impairs IL-4/IL-13 signaling through C/EBP $\beta$ -mediated transcriptional suppression. *J Cell Sci* 126, 4026-4036.
- Bertolotti, A., Zhang, Y., Hendershot, L.M., Harding, H.P., and Ron, D. (2000). Dynamic interaction of BiP and ER stress transducers in the unfolded-protein response. *Nat Cell Biol* 2, 326-332.
- Bright, M.D., Itzhak, D.N., Wardell, C.P., Morgan, G.J., and Davies, F.E. (2015). Cleavage of BLOC1S1 mRNA by IRE1 Is Sequence Specific, Temporally Separate from XBP1 Splicing, and Dispensable for Cell Viability under Acute Endoplasmic Reticulum Stress. *Mol Cell Bio* 35, 2186-2202.
- Calton, M., Zeng, H., Urano, F., Till, J.H., Hubbard, S.R., Harding, H.P., Clark, S.G., and Ron, D. (2002). IRE1 couples endoplasmic reticulum load to secretory capacity by processing the XBP-1 mRNA. *Nature* 415, 92-96.
- Campfield, L.A., Smith, F.J., Guisez, Y., Devos, R., and Burn, P. (1995). Recombinant mouse OB protein: evidence for a peripheral signal linking adiposity and central neural networks. *Science* 269, 546-549.
- Chambers, J.E., Petrova, K., Tomba, G., Vendruscolo, M., and Ron, D. (2012). ADP ribosylation adapts an ER chaperone response to short-term fluctuations in unfolded protein load. *J Cell Biol* 198, 371-385.
- Chen, H., Charlat, O., Tartaglia, L.A., Woolf, E.A., Weng, X., Ellis, S.J., Lakey, N.D., Culpepper, J., Moore, K.J., Breitbart, R.E., Duyk, G.M., Tepper, R.I., and Morgenstern, J.P. (1996). Evidence that the diabetes gene encodes the leptin receptor: identification of a mutation in the leptin receptor gene in db/db mice. *Cell* 84, 491-495.
- Chikka, M.R., McCabe, D.D., Tyra, H.M., and Rutkowski, D.T. (2013). C/EBP homologous protein (CHOP) contributes to suppression of metabolic genes during endoplasmic reticulum stress in the liver. *J Biol Chem* 288, 4405-4415.
- Cinaroglu, A., Gao, C., Imrie, D., and Sadler, K.C. (2011). Activating transcription factor 6 plays protective and pathological roles in steatosis due to endoplasmic reticulum stress in zebrafish. *Hepatology* 54, 495-508.
- Cretenet, G., Le Clech, M., and Gachon, F. (2010). Circadian clock-coordinated 12 Hr period rhythmic activation of the IRE1 $\alpha$  pathway controls lipid metabolism in mouse liver. *Cell Metab* 11, 47-57.

Ezzati, M., Lopez, A.D., Rodgers, A., Vander Hoorn, S., Murray, C.J., and Comparative Risk Assessment Collaborating, G. (2002). Selected major risk factors and global and regional burden of disease. *Lancet* *360*, 1347-1360.

Fan, C., Li, Q., Zhang, Y., Liu, X., Luo, M., Abbott, D., Zhou, W., and Engelhardt, J.F. (2004). I $\kappa$ B $\alpha$  and I $\kappa$ B $\beta$  possess injury context-specific functions that uniquely influence hepatic NF- $\kappa$ B induction and inflammation. *J Clin Invest* *113*, 746-755.

Foufelle, F., and Fromenty, B. (2016). Role of endoplasmic reticulum stress in drug-induced toxicity. *Pharmacol Res Perspect* *4*, e00211.

Gardner, B.M., Pincus, D., Gotthardt, K., Gallagher, C.M., and Walter, P. (2013). Endoplasmic reticulum stress sensing in the unfolded protein response. *Cold Spring Harb Perspect Biol* *5*, a013169.

Gardner, B.M., and Walter, P. (2011). Unfolded proteins are Ire1-activating ligands that directly induce the unfolded protein response. *Science* *333*, 1891-1894.

Gething, M.J. (1999). Role and regulation of the ER chaperone BiP. *Semin Cell Dev Biol* *10*, 465-472.

Gregor, M.F., and Hotamisligil, G.S. (2011). Inflammatory mechanisms in obesity. *Annu Rev Immunol* *29*, 415-445.

Halaas, J.L., Gajiwala, K.S., Maffei, M., Cohen, S.L., Chait, B.T., Rabinowitz, D., Lallone, R.L., Burley, S.K., and Friedman, J.M. (1995). Weight-reducing effects of the plasma protein encoded by the obese gene. *Science* *269*, 543-546.

Han, D., Lerner, A.G., Vande Walle, L., Upton, J.P., Xu, W., Hagen, A., Backes, B.J., Oakes, S.A., and Papa, F.R. (2009). IRE1 $\alpha$  kinase activation modes control alternate endoribonuclease outputs to determine divergent cell fates. *Cell* *138*, 562-575.

Han, D., Upton, J.P., Hagen, A., Callahan, J., Oakes, S.A., and Papa, F.R. (2008). A kinase inhibitor activates the IRE1 $\alpha$  RNase to confer cytoprotection against ER stress. *Biochem Biophys Res Comm* *365*, 777-783.

Harding, H.P., Novoa, I., Zhang, Y., Zeng, H., Wek, R., Schapira, M., and Ron, D. (2000). Regulated translation initiation controls stress-induced gene expression in mammalian cells. *Mol Cell* *6*, 1099-1108.

Harding, H.P., Zhang, Y., and Ron, D. (1999). Protein translation and folding are coupled by an endoplasmic-reticulum-resident kinase. *Nature* *397*, 271-274.

Hollien, J., Lin, J.H., Li, H., Stevens, N., Walter, P., and Weissman, J.S. (2009). Regulated Ire1-dependent decay of messenger RNAs in mammalian cells. *J Cell Biol* *186*, 323-331.

Hollien, J., and Weissman, J.S. (2006). Decay of endoplasmic reticulum-localized mRNAs during the unfolded protein response. *Science* *313*, 104-107.

Hotamisligil, G.S. (2010). Endoplasmic Reticulum Stress and the Inflammatory Basis of Metabolic Disease. *Cell* *140*, 900-917.

Iwakoshi, N.N., Lee, A.H., Vallabhajosyula, P., Otipoby, K.L., Rajewsky, K., and Glimcher, L.H. (2003). Plasma cell differentiation and the unfolded protein response intersect at the transcription factor XBP-1. *Nat Immunol* *4*, 321-329.

Ji, C., Kaplowitz, N., Lau, M.Y., Kao, E., Petrovic, L.M., and Lee, A.S. (2011). Liver-specific loss of glucose-regulated protein 78 perturbs the unfolded protein response and exacerbates a spectrum of liver diseases in mice. *Hepatology* *54*, 229-239.

Kaser, A., Adolph, T.E., and Blumberg, R.S. (2013). The unfolded protein response and gastrointestinal disease. *Semin Immunopathol* *35*, 307-319.

Kawasaki, K., Ushioda, R., Ito, S., Ikeda, K., Masago, Y., and Nagata, K. (2015). Deletion of the collagen-specific molecular chaperone Hsp47 causes endoplasmic reticulum stress-mediated apoptosis of hepatic stellate cells. *J Biol Chem* *290*, 3639-3646.

Kimata, Y., Oikawa, D., Shimizu, Y., Ishiwata-Kimata, Y., and Kohno, K. (2004). A role for BiP as an adjustor for the endoplasmic reticulum stress-sensing protein Ire1. *J Cell Biol* *167*, 445-456.

Lee, A.H., Chu, G.C., Iwakoshi, N.N., and Glimcher, L.H. (2005). XBP-1 is required for biogenesis of cellular secretory machinery of exocrine glands. *EMBO J* *24*, 4368-4380.

Lee, A.H., Iwakoshi, N.N., and Glimcher, L.H. (2003). XBP-1 regulates a subset of endoplasmic reticulum resident chaperone genes in the unfolded protein response. *Mol Cell Bio* *23*, 7448-7459.

Lee, G.H., Proenca, R., Montez, J.M., Carroll, K.M., Darvishzadeh, J.G., Lee, J.I., and Friedman, J.M. (1996). Abnormal splicing of the leptin receptor in diabetic mice. *Nature* *379*, 632-635.

Lee, K., Tirasophon, W., Shen, X., Michalak, M., Prywes, R., Okada, T., Yoshida, H., Mori, K., and Kaufman, R.J. (2002). IRE1-mediated unconventional mRNA splicing and S2P-mediated ATF6 cleavage merge to regulate XBP1 in signaling the unfolded protein response. *Genes Dev* *16*, 452-466.

Lerner, A.G., Upton, J.P., Praveen, P.V., Ghosh, R., Nakagawa, Y., Igbaria, A., Shen, S., Nguyen, V., Backes, B.J., Heiman, M., Heintz, N., Greengard, P., Hui, S., Tang, Q., Trusina, A., Oakes, S.A., and Papa, F.R. (2012). IRE1 $\alpha$  induces thioredoxin-interacting protein to activate the NLRP3 inflammasome and promote programmed cell death under irremediable ER stress. *Cell Metab* *16*, 250-264.

Lin, J.H., Li, H., Yasumura, D., Cohen, H.R., Zhang, C., Panning, B., Shokat, K.M., Lavail, M.M., and Walter, P. (2007). IRE1 signaling affects cell fate during the unfolded protein response. *Science* *318*, 944-949.

Malhi, H., and Kaufman, R.J. (2011). Endoplasmic reticulum stress in liver disease. *J Hepatol* *54*, 795-809.

Marciniak, S.J., Yun, C.Y., Oyadomari, S., Novoa, I., Zhang, Y., Jungreis, R., Nagata, K., Harding, H.P., and Ron, D. (2004). CHOP induces death by promoting protein synthesis and oxidation in the stressed endoplasmic reticulum. *Genes Dev* *18*, 3066-3077.

Maurel, M., Chevet, E., Tavernier, J., and Gerlo, S. (2014). Getting RIDD of RNA: IRE1 in cell fate regulation. *Trends Biochem Sci* *39*, 245-254.

Muse, G.W., Gilchrist, D.A., Nechaev, S., Shah, R., Parker, J.S., Grissom, S.F., Zeitlinger, J., and Adelman, K. (2007). RNA polymerase is poised for activation across the genome. *Nat Genet* *39*, 1507-1511.

- Oyadomari, S., Harding, H.P., Zhang, Y., Oyadomari, M., and Ron, D. (2008). Dephosphorylation of translation initiation factor 2 $\alpha$  enhances glucose tolerance and attenuates hepatosteatosis in mice. *Cell Metab* 7, 520-532.
- Özcan, U., Cao, Q., Yilmaz, E., Lee, A.-H., Iwakoshi, N.N., Özdelen, E., Tuncman, G., Görgün, C., Glimcher, L.H., and Hotamisligil, G.S. (2004). Endoplasmic Reticulum Stress Links Obesity, Insulin Action, and Type 2 Diabetes. *Science* 306, 457-461.
- Özcan, U., Özcan, L., Yilmaz, E., Duvel, K., Sahin, M., Manning, B.D., and Hotamisligil, G.S. (2008). Loss of the tuberous sclerosis complex tumor suppressors triggers the unfolded protein response to regulate insulin signaling and apoptosis. *Mol Cell* 29, 541-551.
- Özcan, U., Yilmaz, E., Özcan, L., Furuhashi, M., Vaillancourt, E., Smith, R.O., Görgün, C.Z., and Hotamisligil, G.S. (2006). Chemical Chaperones Reduce ER Stress and Restore Glucose Homeostasis in a Mouse Model of Type 2 Diabetes. *Science* 313, 1137-1140.
- Pelleymounter, M.A., Cullen, M.J., Baker, M.B., Hecht, R., Winters, D., Boone, T., and Collins, F. (1995). Effects of the obese gene product on body weight regulation in ob/ob mice. *Science* 269, 540-543.
- Pfaffenbach, K.T., Nivala, A.M., Reese, L., Ellis, F., Wang, D., Wei, Y., and Pagliassotti, M.J. (2010). Rapamycin inhibits postprandial-mediated X-box-binding protein-1 splicing in rat liver. *J Nutr* 140, 879-884.
- Preissler, S., Rato, C., Chen, R., Antrobus, R., Ding, S., Fearnley, I.M., and Ron, D. (2015). AMPylation matches BiP activity to client protein load in the endoplasmic reticulum. *eLife* 4, e12621.
- Resendez, E., Jr., Wooden, S.K., and Lee, A.S. (1988). Identification of highly conserved regulatory domains and protein-binding sites in the promoters of the rat and human genes encoding the stress-inducible 78-kilodalton glucose-regulated protein. *Mol Cell Bio* 8, 4579-4584.
- Rutkowski, D.T., Arnold, S.M., Miller, C.N., Wu, J., Li, J., Gunnison, K.M., Mori, K., Sadighi Akha, A.A., Raden, D., and Kaufman, R.J. (2006). Adaptation to ER stress is mediated by differential stabilities of pro-survival and pro-apoptotic mRNAs and proteins. *PLoS Biol* 4, e374.
- Rutkowski, D.T., Wu, J., Back, S.H., Callaghan, M.U., Ferris, S.P., Iqbal, J., Clark, R., Miao, H., Hassler, J.R., Fornek, J., Katze, M.G., Hussain, M.M., Song, B., Swathirajan, J., Wang, J., Yau, G.D., and Kaufman, R.J. (2008). UPR pathways combine to prevent hepatic steatosis caused by ER stress-mediated suppression of transcriptional master regulators. *Dev Cell* 15, 829-840.
- Sano, R., and Reed, J.C. (2013). ER stress-induced cell death mechanisms. *Biochim Biophys Acta* 1833, 3460-3470.
- Shao, M., Shan, B., Liu, Y., Deng, Y., Yan, C., Wu, Y., Mao, T., Qiu, Y., Zhou, Y., Jiang, S., Jia, W., Li, J., Li, J., Rui, L., Yang, L., and Liu, Y. (2014). Hepatic IRE1 $\alpha$  regulates fasting-induced metabolic adaptive programs through the XBP1s-PPAR $\alpha$  axis signalling. *Nat Commun* 5, 3528.
- Shen, J., Chen, X., Hendershot, L., and Prywes, R. (2002). ER stress regulation of ATF6 localization by dissociation of BiP/GRP78 binding and unmasking of golgi localization signals. *Dev Cell* 3, 99-111.

- Shi, Y., Vattem, K.M., Sood, R., An, J., Liang, J., Stramm, L., and Wek, R.C. (1998). Identification and characterization of pancreatic eukaryotic initiation factor 2 alpha-subunit kinase, PEK, involved in translational control. *Mol Cell Bio* *18*, 7499-7509.
- So, J.S., Hur, K.Y., Tarrio, M., Ruda, V., Frank-Kamenetsky, M., Fitzgerald, K., Koteliensky, V., Lichtman, A.H., Iwawaki, T., Glimcher, L.H., and Lee, A.H. (2012). Silencing of lipid metabolism genes through IRE1alpha-mediated mRNA decay lowers plasma lipids in mice. *Cell Metab* *16*, 487-499.
- Tyra, H.M., Spitz, D.R., and Rutkowski, D.T. (2012). Inhibition of fatty acid oxidation enhances oxidative protein folding and protects hepatocytes from endoplasmic reticulum stress. *Mol Biol Cell* *23*, 811-819.
- Upton, J.P., Wang, L., Han, D., Wang, E.S., Huskey, N.E., Lim, L., Truitt, M., McManus, M.T., Ruggero, D., Goga, A., Papa, F.R., and Oakes, S.A. (2012). IRE1alpha cleaves select microRNAs during ER stress to derepress translation of proapoptotic Caspase-2. *Science* *338*, 818-822.
- van Anken, E., Romijn, E.P., Maggioni, C., Mezghrani, A., Sitia, R., Braakman, I., and Heck, A.J. (2003). Sequential waves of functionally related proteins are expressed when B cells prepare for antibody secretion. *Immunity* *18*, 243-253.
- Walter, P., and Ron, D. (2011). The unfolded protein response: from stress pathway to homeostatic regulation. *Science* *334*, 1081-1086.
- Wu, J., Rutkowski, D.T., Dubois, M., Swathirajan, J., Saunders, T., Wang, J., Song, B., Yau, G.D., and Kaufman, R.J. (2007). ATF6alpha optimizes long-term endoplasmic reticulum function to protect cells from chronic stress. *Dev Cell* *13*, 351-364.
- Yamamoto, K., Takahara, K., Oyadomari, S., Okada, T., Sato, T., Harada, A., and Mori, K. (2010). Induction of liver steatosis and lipid droplet formation in ATF6alpha-knockout mice burdened with pharmacological endoplasmic reticulum stress. *Mol Biol Cell* *21*, 2975-2986.
- Yamamoto, K., Yoshida, H., Kokame, K., Kaufman, R.J., and Mori, K. (2004). Differential contributions of ATF6 and XBP1 to the activation of endoplasmic reticulum stress-responsive cis-acting elements ERSE, UPRE and ERSE-II. *J Biochem* *136*, 343-350.
- Yanagitani, K., Imagawa, Y., Iwawaki, T., Hosoda, A., Saito, M., Kimata, Y., and Kohno, K. (2009). Cotranslational Targeting of XBP1 Protein to the Membrane Promotes Cytoplasmic Splicing of Its Own mRNA. *Mol Cell* *34*, 191-200.
- Yang, L., Calay, E.S., Fan, J., Arduini, A., Kunz, R.C., Gygi, S.P., Yalcin, A., Fu, S., and Hotamisligil, G.S. (2015). S-Nitrosylation links obesity-associated inflammation to endoplasmic reticulum dysfunction. *Science* *349*, 500-506.
- Ye, J., Rawson, R.B., Komuro, R., Chen, X., Dave, U.P., Prywes, R., Brown, M.S., and Goldstein, J.L. (2000). ER stress induces cleavage of membrane-bound ATF6 by the same proteases that process SREBPs. *Mol Cell* *6*, 1355-1364.
- Yoshida, H., Haze, K., Yanagi, H., Yura, T., and Mori, K. (1998). Identification of the cis-acting endoplasmic reticulum stress response element responsible for transcriptional induction of mammalian glucose-regulated proteins. Involvement of basic leucine zipper transcription factors. *J Biol Chem* *273*, 33741-33749.

Yoshida, H., Matsui, T., Yamamoto, A., Okada, T., and Mori, K. (2001). XBP1 mRNA is induced by ATF6 and spliced by IRE1 in response to ER stress to produce a highly active transcription factor. *Cell* *107*, 881-891.

Young, C.N., Cao, X., Guraju, M.R., Pierce, J.P., Morgan, D.A., Wang, G., Iadecola, C., Mark, A.L., and Davisson, R.L. (2012). ER stress in the brain subfornical organ mediates angiotensin-dependent hypertension. *J Clin Invest* *122*, 3960-3964.

Young, C.N., and Davisson, R.L. (2015). Angiotensin-II, the Brain, and Hypertension: An Update. *Hypertension* *66*, 920-926.

Zhang, K., Shen, X., Wu, J., Sakaki, K., Saunders, T., Rutkowski, D.T., Back, S.H., and Kaufman, R.J. (2006). Endoplasmic reticulum stress activates cleavage of CREBH to induce a systemic inflammatory response. *Cell* *124*, 587-599.

Zhang, K., Wang, S., Malhotra, J., Hassler, J.R., Back, S.H., Wang, G., Chang, L., Xu, W., Miao, H., Leonardi, R., Chen, Y.E., Jackowski, S., and Kaufman, R.J. (2011). The unfolded protein response transducer IRE1 $\alpha$  prevents ER stress-induced hepatic steatosis. *EMBO J* *30*, 1357-1375.

Zhou, A.X., and Tabas, I. (2013). The UPR in atherosclerosis. *Semin Immunopathol* *35*, 321-332.

Zinszner, H., Kuroda, M., Wang, X., Batchvarova, N., Lightfoot, R.T., Remotti, H., Stevens, J.L., and Ron, D. (1998). CHOP is implicated in programmed cell death in response to impaired function of the endoplasmic reticulum. *Genes Dev* *12*, 982-995.

Zode, G.S., Kuehn, M.H., Nishimura, D.Y., Searby, C.C., Mohan, K., Grozdanic, S.D., Bugge, K., Anderson, M.G., Clark, A.F., Stone, E.M., and Sheffield, V.C. (2011). Reduction of ER stress via a chemical chaperone prevents disease phenotypes in a mouse model of primary open angle glaucoma. *J Clin Invest* *121*, 3542-3553.



Figure 1, Gomez et al.

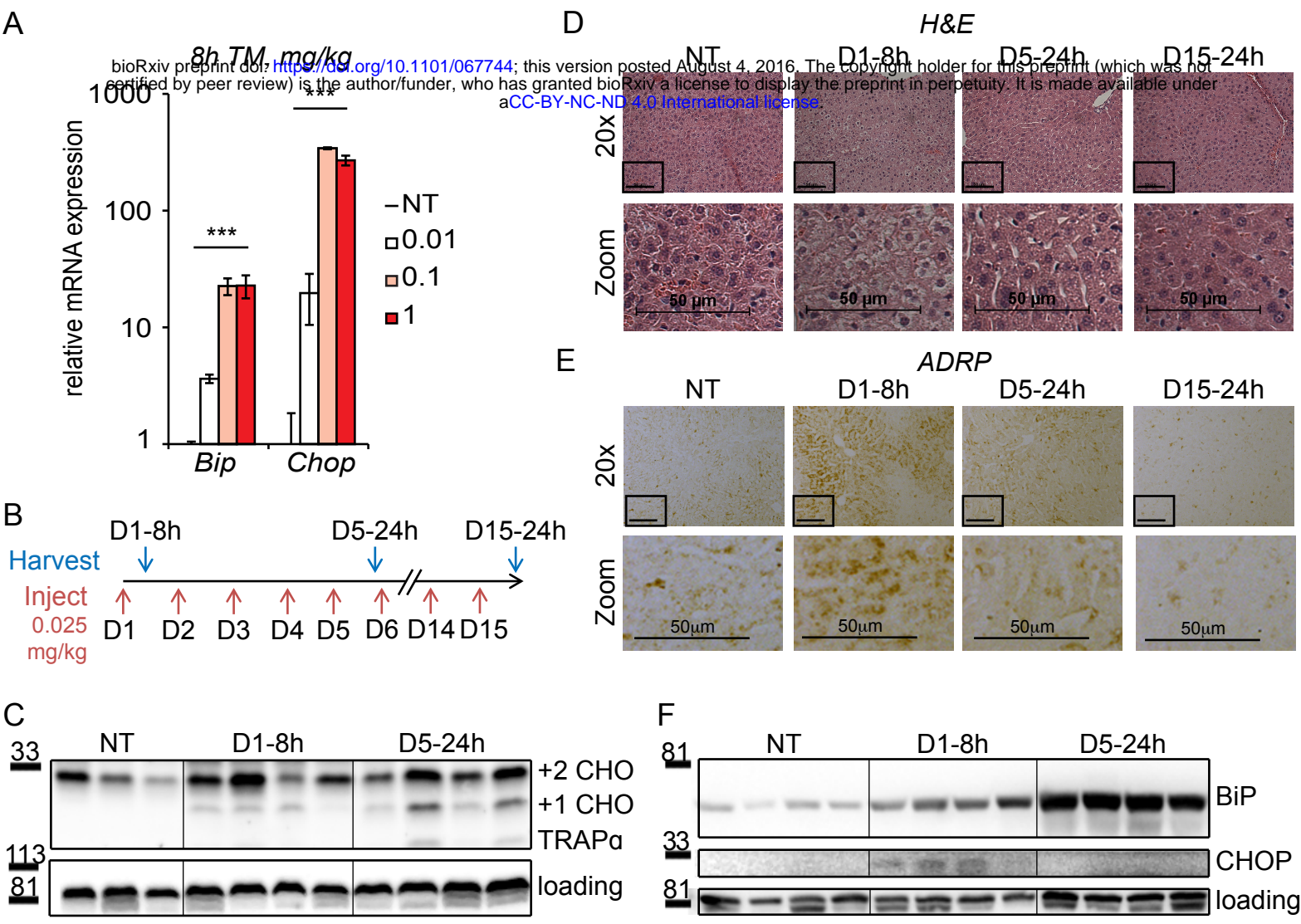




Figure 2, Gomez et al.

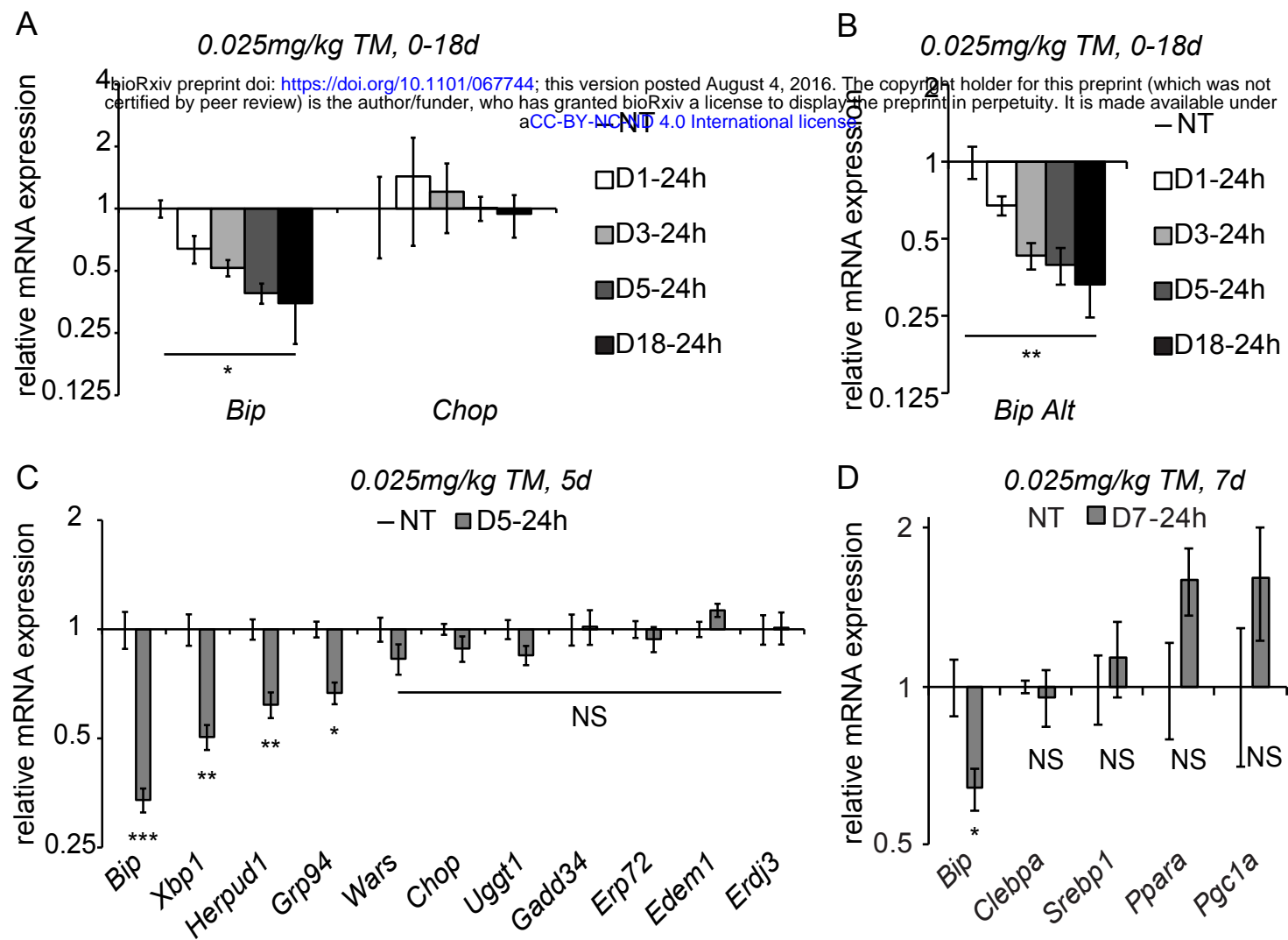


Figure 3, Gomez et al.

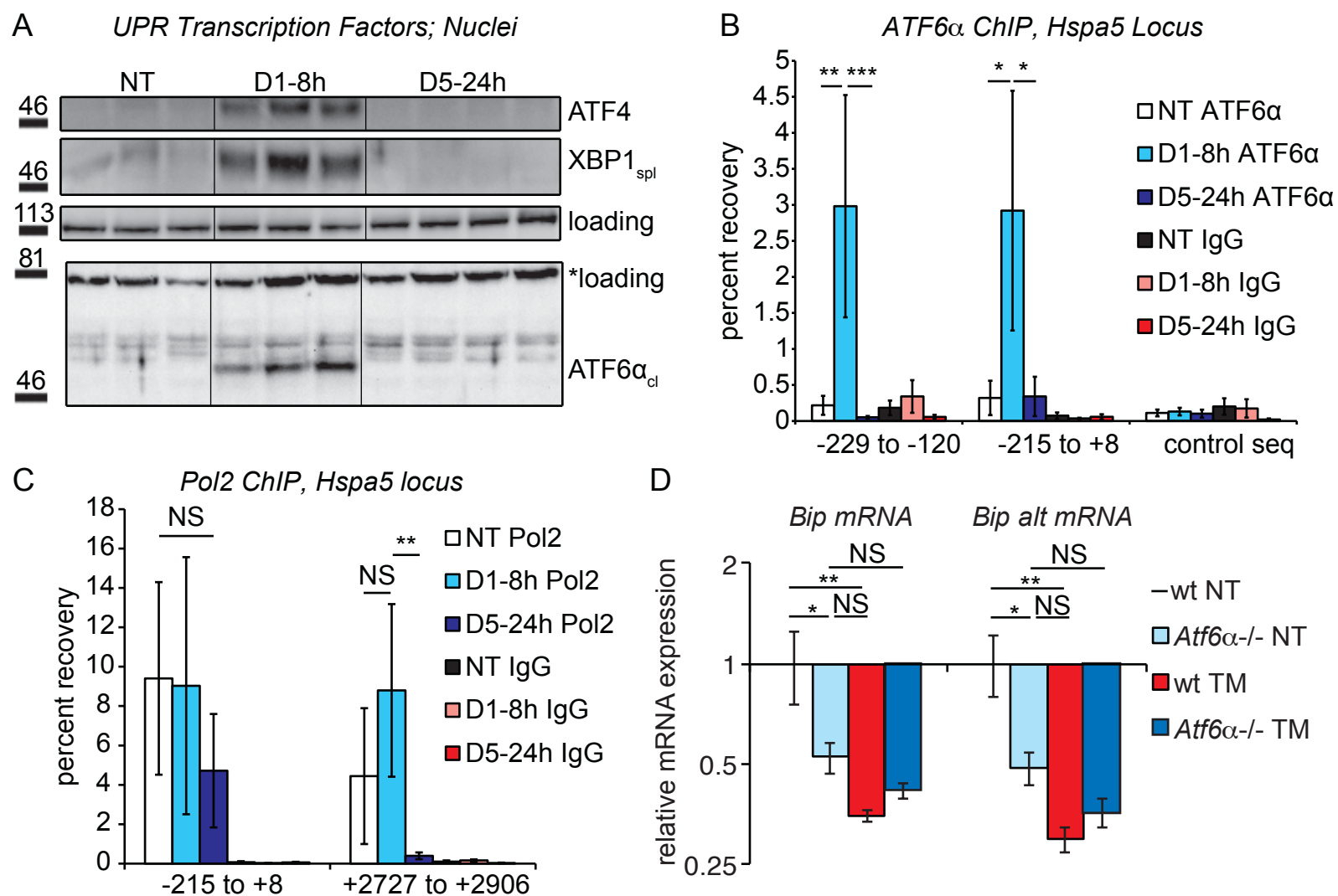
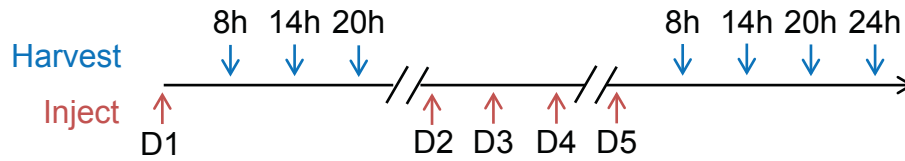
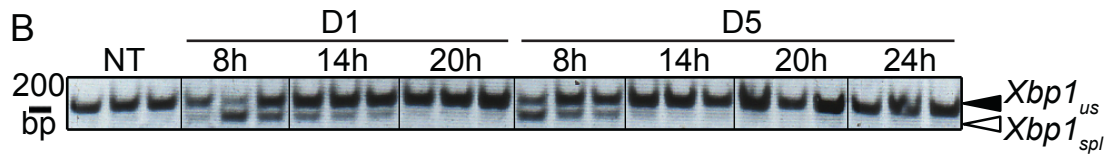


Figure 4, Gomez et al.

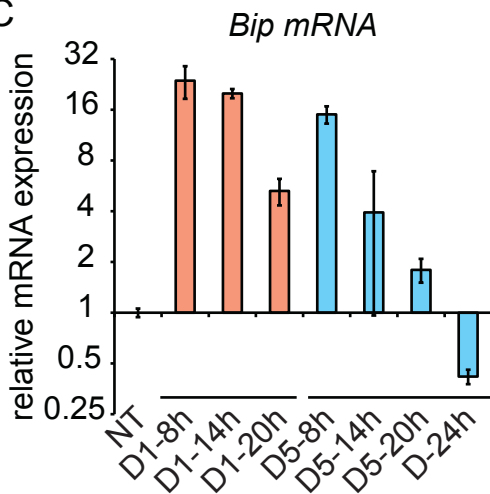
A



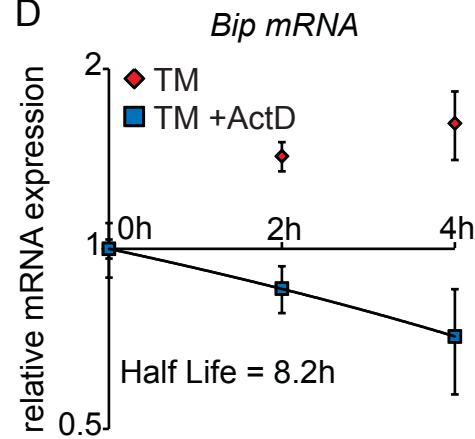
B



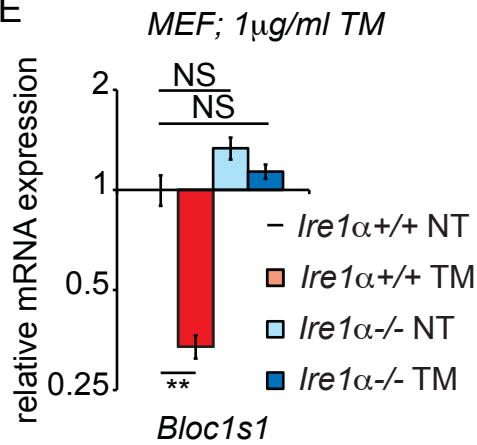
C



D



E



F

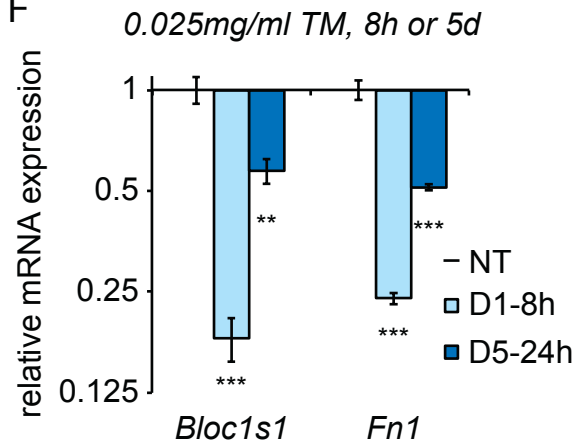


Figure 5, Gomez et al.

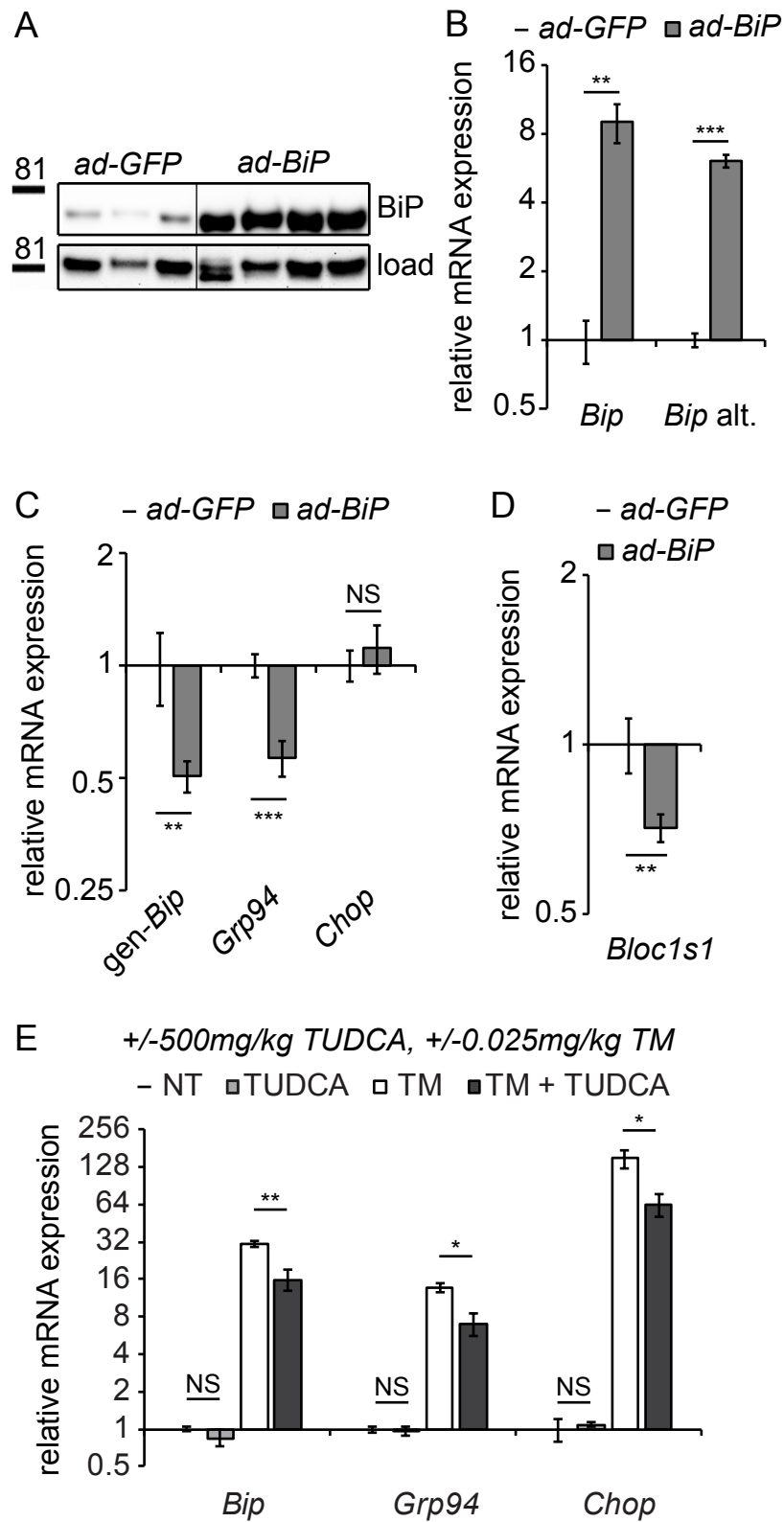


Figure 6, Gomez et al.

